Electromagnetic Forces Acting on the Planar Armature of a Core-Type Synchronous Permanent-Magnet Planar Motor

Jiayong Cao[1], Yu Zhu[2], Wensheng Yin[2], and Wei Xu[1]

[1]School of Mechanical Engineering, Shanghai Jiao Tong University, Shanghai 200240, China
[2]Department of Precision Instruments & Mechanology, Tsinghua University, Beijing 100084, China

The core-type synchronous permanent-magnet planar motor (SPMPM) discussed in this paper includes one or more planar armatures each of which contains two sets of three-phase windings named x-winding and y-winding. For each planar armature, a magnetic field energy equation is established first. This equation describes the mechanism of the coupling between the permanent-magnet array, the x-winding and the y-winding in the core-type SPMPM. By using virtual work principle, x-direction thrust force, y-direction thrust force and vertical force acting on the planar armature are modeling analytically. For eliminating the coupling in these force models, the excitation flux linkages and phase currents are all transformed into d-q synchronous reference frame. From the decoupling force equations, some characteristics of the vertical component of force on the planar armature are obtained. The electromagnetic force model is helpful for the design of the contactless planar bearing and the servo control system of the SPMPM.

***Index Terms*—Iron core, magnetic field energy, permanent magnet, planar motor, reference frame transformation, virtual work force.**

I. INTRODUCTION

In contrast to the induction planar motor and variable reluctance planar motor, the synchronous permanent-magnet planar motor (SPMPM) has the advantages of low thrust ripple, high efficiency, and capability of being designed for low speed [1]–[9], [13]. According to whether or not the armature have iron core or not, the SPMPM can be classified into core and coreless (or ironless) types [4]. The core-type SPMPM has some benefits such as higher power and larger thrust, because the peak air-gap flux density of the core-type SPMPM is much higher than that in the coreless SPMPM.

However, in the core-type SPMPM, the attraction force acting on the mover is very large. It may lead to serious abrasion if a contact-type planar bearing is used. Hence, the utilization of some type of contactless planar bearings such as planar air bearings or planar magnet bearings is very helpful. The levitation force produced by the contactless planar bearing can balance the vertical gravity force and the attraction force acting on the mover very well. However, a good design of the contactless planar bearing is difficult to be realized if the vertical attraction force acting on the mover is not estimated precisely.

In this paper, an analytical model for calculating the vertical electromagnetic force F_{v} in a core-type SPMPM is proposed. This core-type SPMPM is shown in Fig. 1, which has been discussed in [5]. Every planar armature includes two sets of windings called x-winding and y-winding, which are corresponding to x-direction thrust force F_{x} and y-direction thrust force F_{y}, respectively. Another topic of this paper is to discuss the analytical model of x-direction thrust force F_{x} and y-direction thrust force F_{y}. Both topics are based on a modified magnetic field energy equation.

Manuscript received January 10, 2007; revised July 28, 2008 and November 05, 2008. Current version published July 22, 2009. Corresponding author: J. Cao (e-mail: caojy@sjtu.edu.cn).

Color versions of one or more of the figures in this paper are available online at http://ieeexplore.ieee.org.

Digital Object Identifier 10.1109/TMAG.2009.2023365

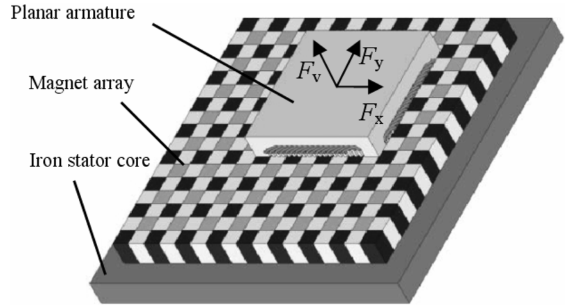

Fig. 1. Outline drawing of a core-type SPMPM.

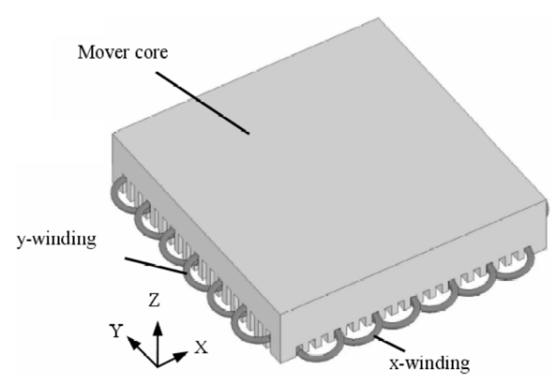

Fig. 2. Mover core and winding configuration.

II. A MODIFIED MAGNETIC FIELD ENERGY EQUATION FLUX DENSITY EQUATIONS

For clarity, some assumptions to be used below are given first: 1) the magnetic saturation in the iron cores is little enough to be neglected, i.e., the magnetic field has linear property; 2) the end effect can be neglected; and 3) the flux leakage is small enough to be neglected.

The core-type SPMPM discussed in this paper is an electromechanical system including three electrical parts: magnet array part, x-winding part, and y-winding part. There are six electrical ports and three mechanical ports in this system. The inputs of the electrical ports are the phase currents of x-winding and y-winding which can be expressed as two vectors:

$$\boldsymbol{I}_{\rm x} = [\, i_{\rm a}^{\rm x} \quad i_{\rm b}^{\rm x} \quad i_{\rm c}^{\rm x} \,]^{\rm T}, \quad \boldsymbol{I}_{\rm y} = [\, i_{\rm a}^{\rm y} \quad i_{\rm b}^{\rm y} \quad i_{\rm c}^{\rm y} \,]^{\rm T} \tag{1}$$

Due to the linear magnetic material, the magnetic field energy (MFE) $W_{\rm f}$ of the core-type SPMPM can be expressed as follows:

$$W_{\rm f} = \frac{1}{2}\mathbf{I}_{\rm x}^{\rm t}\mathbf{L}_{\rm x}\mathbf{I}_{\rm x} + \frac{1}{2}\mathbf{I}_{\rm y}^{\rm t}\mathbf{L}_{\rm y}\mathbf{I}_{\rm y} + \frac{1}{2}\mathbf{I}_{\rm x}^{\rm t}\mathbf{M}_{\rm xy}\mathbf{I}_{\rm y} + \frac{1}{2}\mathbf{I}_{\rm y}^{\rm t}\mathbf{M}_{\rm yx}\mathbf{I}_{\rm x} + \mathbf{I}_{\rm x}^{\rm t}\boldsymbol{\psi}_{\rm e}^{\rm x} + \mathbf{I}_{\rm y}^{\rm t}\boldsymbol{\psi}_{\rm e}^{\rm y} + W_{\rm fa} \tag{2}$$

where $W_{\rm fa}$ is the magnetic field energy component generated by the permanent-magnet array, $\boldsymbol{L}_{\rm x}$ and $\boldsymbol{L}_{\rm y}$ are inductance matrices of x-windings and y-windings, $\boldsymbol{M}_{\rm xy}$ and $\boldsymbol{M}_{\rm yx}$ are the matrices of mutual inductances between x-windings and y-windings, $\psi_{\rm e}^{\rm x}$ and $\psi_{\rm e}^{\rm y}$ are the vectors of excitation flux linkage linking x-windings and y-windings. The detailed forms of the above matrices or vectors are

$$\boldsymbol{\psi}_{\rm e}^{\rm x} = [\, \psi_{\rm ea}^{\rm x} \quad \psi_{\rm eb}^{\rm x} \quad \psi_{\rm ec}^{\rm x} \,]^{\rm T}, \ \boldsymbol{\psi}_{\rm e}^{\rm y} = [\, \psi_{\rm ea}^{\rm y} \quad \psi_{\rm eb}^{\rm y} \quad \psi_{\rm ec}^{\rm y} \,]^{\rm T}$$
$$\boldsymbol{L}_{\rm x} = \begin{bmatrix} L_{\rm aa}^{\rm x} & L_{\rm ab}^{\rm x} & L_{\rm ac}^{\rm x} \\ L_{\rm ba}^{\rm x} & L_{\rm bb}^{\rm x} & L_{\rm bc}^{\rm x} \\ L_{\rm ca}^{\rm x} & L_{\rm bc}^{\rm x} & L_{\rm cc}^{\rm x} \end{bmatrix}, \ \boldsymbol{L}_{\rm y} = \begin{bmatrix} L_{\rm aa}^{\rm y} & L_{\rm ab}^{\rm y} & L_{\rm ac}^{\rm y} \\ L_{\rm ba}^{\rm y} & L_{\rm bb}^{\rm y} & L_{\rm bc}^{\rm y} \\ L_{\rm ca}^{\rm y} & L_{\rm cb}^{\rm y} & L_{\rm cc}^{\rm y} \end{bmatrix}$$
$$\boldsymbol{M}_{\rm xy} = \begin{bmatrix} M_{\rm xaya} & M_{\rm xayb} & M_{\rm xayc} \\ M_{\rm xbya} & M_{\rm xbyb} & M_{\rm xbyc} \\ M_{\rm xcya} & M_{\rm xcyb} & M_{\rm xcyc} \end{bmatrix}, \ \boldsymbol{M}_{\rm yx} = \boldsymbol{M}_{\rm xy}$$

where subscript or superscript x and y denote x-windings and y-windings, subscript a, b, and c denote phase A, phase B, and phase C of x-windings or y-windings. In (2), the term of $W_{\rm fa}$ which describes the component of static magnetic field appears. However this term is neglected before [5]. Therefore, the magnetic field (2) is more exact than that proposed before. In [5], the characteristics of $M_{\rm xy}$ and $M_{\rm yx}$ were analyzed. The conclusion is that $M_{\rm xy} = M_{\rm yx} = 0$. Thus, the MFE equation (2) can be simplified as

$$W_{\rm f} = \frac{1}{2}\boldsymbol{I}_{\rm x}^{\rm t}\boldsymbol{L}_{\rm x}\boldsymbol{I}_{\rm x} + \frac{1}{2}\boldsymbol{I}_{\rm y}^{\rm t}\boldsymbol{L}_{\rm y}\boldsymbol{I}_{\rm y} + \boldsymbol{I}_{\rm x}^{\rm t}\boldsymbol{\psi}_{\rm e}^{\rm x} + \boldsymbol{I}_{\rm y}^{\rm t}\boldsymbol{\psi}_{\rm e}^{\rm y} + W_{\rm fa}. \tag{3}$$

According to electric machine theory, the concentrated-winding model is equivalent to a sine-distributed winding model when a fundamental winding coefficient is taken. Being similar to the principle of analyzing the induction matrix of the rotary electric motors [5], [11], the approach to calculate the inductions of the core-type SPMPM can be obtained:

$$L_{\rm aa}^{\rm x} = L_{\rm bb}^{\rm x} = L_{\rm cc}^{\rm x} = L_{\rm ph} \tag{4}$$
$$L_{\rm aa}^{\rm y} = L_{\rm bb}^{\rm y} = L_{\rm cc}^{\rm y} = L_{\rm ph} \tag{5}$$
$$L_{\rm ab}^{\rm x} = L_{\rm ac}^{\rm x} = L_{\rm bc}^{\rm x} = L_{\rm ba}^{\rm x} = L_{\rm ca}^{\rm x} = L_{\rm cb}^{\rm x} = -L_{\rm ph}/2 \tag{6}$$
$$L_{\rm ab}^{\rm y} = L_{\rm ac}^{\rm y} = L_{\rm bc}^{\rm y} = L_{\rm ba}^{\rm y} = L_{\rm ca}^{\rm y} = L_{\rm bc}^{\rm y} = -L_{\rm ph}/2 \tag{7}$$
$$L_{\rm ph} = \frac{\mu_0 \tau l N_{\rm s}^2}{4g''p} \tag{8}$$

where μ_0 is the vacuum permeability, τ is width of each permanent magnet (i.e., half of the pitch of the magnet array), $l_{\rm m}$ is the height of the permanent magnets, p is the number of pole pair of the x-winding and y-winding. $N_{\rm s} = 4K_1N_{\rm ph}/\pi$ is the equivalent sine-distributed series turns per phase for the fundamental, K_1 is fundamental winding coefficient, $N_{\rm ph}$ is the number of turns in series per phase, l is the length of the mover core, and g'' is named as equivalent air gap thickness.

The definition of g'' is the same with that of the classic electric machine theory. For the SPMPM in which some iron pieces embbed into the magnet array, g'' can be calculated by using the following equation:

$$g'' = K_{c1}g + K_{c2}l_m \tag{9}$$

where $K_{\rm c1}$ is Carter's coefficient corresponding to mover teeth, $K_{\rm c2}$ is Carter's coefficient corresponding to stator teeth. For the SPMPM with surface magnet array, there are no iron pieces embedded into the magnet array. Therefore, Carter's effect corresponding to stator teeth can be neglected, i.e., $K_{\rm c2} = 1$.

In [5], the equations for calculating and have been given:

$$\boldsymbol{\psi}_{\rm e}^{\rm x} = \psi_m \left[\cos(\theta_{\rm x}) \quad \cos\left(\theta_{\rm x} - \tfrac{2}{3}\pi\right) \quad \cos\left(\theta_{\rm x} + \tfrac{2}{3}\pi\right)\right]^{\rm T} \tag{10}$$
$$\boldsymbol{\psi}_{\rm e}^{\rm y} = \psi_m \left[\cos(\theta_{\rm y}) \quad \cos\left(\theta_{\rm y} - \tfrac{2}{3}\pi\right) \quad \cos\left(\theta_{\rm y} + \tfrac{2}{3}\pi\right)\right]^{\rm T} \tag{11}$$

where $\theta_{\rm x} = \pi x/\tau$ and $\theta_{\rm y} = \pi y/\tau$ is the electric angles, $N_{\rm x}$ and $N_{\rm y}$ are the number of turns in series per phase of x-winding and y-winding, respectively, and $l_{\rm x}$ and $l_{\rm y}$ are the x-direction length and y-direction length of the armature iron core, respectively, $\psi_{\rm m} = 2\,\tau N_{\rm x} l_{\rm y} B_{\rm P}/\pi$, and $B_{\rm p}$ is given by

$$B_{\rm p} = \frac{2B_{\rm r}\sinh(a_1 l_m)}{\mu_{\rm mr}{\rm sch}_1}.$$

In fact, $B_{\rm p}$ is approximately equal to the half of the peak flux density in the bottom plane of the mover core, because from (31) we can obtain

$$B_{\rm z}|_{z=l_{gm}} \approx B_{\rm p}[\sin(a_1x) + \sin(a_1y)]$$

where

$${\rm sch}_1 = \mu_{\rm mr}\sinh(a_1g)\cosh(a_1l_m) + \cosh(a_1g)\sinh(a_1l_m),$$
$$l_{\rm gm} = g + l_m, \quad a_1 = \pi/\tau.$$

In the Appendix, the magnetic field energy of permanent-magnet array $W_{\rm fa}$ is analyzed. It is found that $W_{\rm fa}$ is independent of the mover center position (x,y) and is the unary function of the air-gap thickness g. The expression of this function is

$$W_{\rm fa} = \sum_{k=1,3,\ldots}^{\infty} W_{{\rm fa}k} = \sum_{k=1,3,\ldots}^{\infty} \mu_0 l^2 \left(\frac{M_k^2 l_{\rm m}}{2\mu_{\rm mr}} - \frac{M_k^2 \sinh(a_k g)\sinh(a_k l_{\rm m})}{2a_k{\rm sch}_k}\right) \tag{12}$$

where $\mu_{\rm mr}$ is the relative permeability of the permanent-magnet material, and

$$\begin{aligned}\mathrm{sch}_k &= \mu_{\rm mr}\sinh(a_k g)\cosh(a_k l_m)\\ &\quad + \cosh(a_k g)\sinh(a_k l_m), \quad k=1,3,5,\ldots\\ a_k &= k\pi/\tau, \quad k=1,3,5,\ldots.\end{aligned}$$

In addition, M_k is the coefficient of the Fourier series expansion of the magnetization function of the magnet array [1]

$$M_k = \frac{2B_{\rm r}}{\mu_0\pi}\frac{1}{k}, \quad k=1,3,5,\ldots$$

where $B_{\rm r}$ is the residual flux density of the permanent-magnet material.

III. Lateral Thrust Forces Equation

Because for linear system, co-energy $W_{\rm c}$ is equal to magnetic field energy $W_{\rm f}$, the x-direction electromagnetic thrust can be calculated by the virtual work principle

$$F_{\rm x} = \left.\frac{\partial W_{\rm c}}{\partial x}\right|_{\mathbf{I}_{\rm x}=\text{const},\mathbf{I}_{\rm y}=\text{const}} = \left.\frac{\partial W_{\rm f}}{\partial x}\right|_{\mathbf{I}_{\rm x}=\text{const},\mathbf{I}_{\rm y}=\text{const}}. \tag{13}$$

It has been concluded in Section II that $\boldsymbol{L}_{\rm x}$ and $\boldsymbol{L}_{\rm y}$ are constant matrixes and $W_{\rm fa}$ is independent of the mover center position (x,y). According to magnetic circuit theory, [5] points out that $\boldsymbol{\psi}_{\rm e}^{\rm x}$ and $\boldsymbol{\psi}_{\rm e}^{\rm y}$ are unary functions of y and x, respectively [5]. Therefore, substituting (3) into (13) yields

$$F_{\rm x} = \frac{\partial W_{\rm f}}{\partial x} = (\mathbf{I}_{\rm x})^{\rm t}\frac{\partial}{\partial x}\boldsymbol{\psi}_{\rm e}^{\rm x}.$$

By defining the d-q-0 synchronous transformation matrix $\boldsymbol{K}_{\rm x}(\theta_{\rm x})$, the following transformation relationship is obtained:

$$\boldsymbol{I}_{\rm dq0}^{\rm x} = [\,i_{\rm d}^{\rm x} \quad i_{\rm q}^{\rm x} \quad i_0^{\rm x}\,]^{\rm t} = \boldsymbol{K}_{\rm x}(\theta_{\rm x})\boldsymbol{I}_{\rm x} \tag{14}$$

$$\boldsymbol{\psi}_{\rm e,dq0}^{\rm x} = [\,\psi_{\rm d}^{\rm x} \quad \psi_{\rm q}^{\rm x} \quad \psi_0^{\rm x}\,]^{\rm t} = \boldsymbol{K}_{\rm x}(\theta_{\rm x})\boldsymbol{\psi}_{\rm e}^{\rm x}. \tag{15}$$

The following equation can be derived:

$$F_{\rm x} = \frac{\pi}{\tau}\left(\mathbf{I}_{\rm dq0}^{\rm x}\right)^{\rm t}\left(\mathbf{K}_{\rm x}^{-1}\right)^{\rm t}\frac{\partial}{\partial\theta_{\rm x}}\left(\mathbf{K}_{\rm x}^{-1}\right)\boldsymbol{\psi}_{\rm e,dq0}^{\rm x} \tag{16}$$

where $\theta_{\rm x} = \pi x/\tau$ is the electric angle.

Since

$$\left(\mathbf{K}_{\rm x}^{-1}\right)^{\rm t}\frac{\partial}{\partial\theta_{\rm x}}\left(\mathbf{K}_{\rm x}^{-1}\right) = \begin{bmatrix}0 & -3/2 & 0\\ 3/2 & 0 & 0\\ 0 & 0 & 0\end{bmatrix}.$$

If the d-axis is fixed on the axis of the magnetic pole, (15) can be simplified as

$$\boldsymbol{\psi}_{\rm e,dq0}^{\rm x} = [\,\psi_{\rm e,d}^{\rm x} \quad \psi_{\rm e,q}^{\rm x} \quad \psi_{\rm e,0}^{\rm x}\,]^{\rm t} = [\,\psi_m \quad 0 \quad \psi_{\rm e,0}^{\rm x}\,]^{\rm t}.$$

Then (16) can be rewritten as

$$F_{\rm x} = \frac{3}{2}\frac{\pi}{\tau}i_{\rm q}^{\rm x}\psi_{\rm m}. \tag{17}$$

For y-windings, the similar expressions can also be obtained:

$$F_{\rm y} = \frac{3}{2}\frac{\pi}{\tau}i_{\rm q}^{\rm y}\psi_{\rm m}. \tag{18}$$

IV. Vertical Force Equation

According to the virtual work principle

$$\begin{aligned}F_{\rm v} &= \left.\frac{\partial W_{\rm f}}{\partial g}\right|_{\boldsymbol{I}_{\rm x}=\text{const},\boldsymbol{I}_{\rm y}=\text{const}}\\ &= \frac{1}{2}\boldsymbol{I}_{\rm x}^{\rm t}\frac{\partial}{\partial g}\boldsymbol{L}_{\rm x}\boldsymbol{I}_{\rm x} + \frac{1}{2}\boldsymbol{I}_{\rm y}^{\rm t}\frac{\partial}{\partial g}\boldsymbol{L}_{\rm y}\boldsymbol{I}_{\rm y}\\ &\quad + \boldsymbol{I}_{\rm x}^{\rm t}\frac{\partial}{\partial g}\boldsymbol{\psi}_{\rm f}^{\rm x} + \boldsymbol{I}_{\rm x}^{\rm t}\frac{\partial}{\partial g}\boldsymbol{\psi}_{\rm f}^{\rm y} + \frac{\partial}{\partial g}W_{\rm fa}.\end{aligned} \tag{19}$$

From (4)–(9), we obtain

$$\frac{\partial}{\partial g}\boldsymbol{L}_{\rm x} = \frac{\partial}{\partial g}\boldsymbol{L}_{\rm y} = \frac{\partial L_{\rm ph}}{\partial g}\boldsymbol{\Gamma} \tag{20}$$

where

$$\begin{aligned}\frac{\partial L_{\rm ph}}{\partial g} &= \frac{-K_{c1}\mu_0\tau l N_{\rm s}^2}{4p\left(K_{c1}g + K_{c2}l_m\right)^2}\\ \boldsymbol{\Gamma} &= \begin{bmatrix}1 & -1/2 & -1/2\\ -1/2 & 1 & -1/2\\ -1/2 & -1/2 & 1\end{bmatrix}.\end{aligned} \tag{21}$$

In this paper, $N_{\rm x} = N_{\rm y} = N_{\rm ph}$ and $l_{\rm x} = l_{\rm y} = l = 2k\tau, k > 1$. Hence, the partial derivatives of (10) and (11) with respect to the variable g are represented as

$$\begin{aligned}\frac{\partial}{\partial g}\boldsymbol{\psi}_{\rm e}^{\rm x} &= \frac{1}{\pi}\tau N l\frac{\partial B_{\rm p}}{\partial g}\\ &\quad\times\left[\cos(\theta_{\rm x}) \quad \cos\left(\theta_{\rm x} - \tfrac{2}{3}\pi\right) \quad \cos\left(\theta_{\rm x} - \tfrac{4}{3}\pi\right)\right]^{\rm T}\end{aligned} \tag{22}$$

$$\begin{aligned}\frac{\partial}{\partial g}\boldsymbol{\psi}_{\rm e}^{\rm y} &= \frac{1}{\pi}\tau N l\frac{\partial B_{\rm p}}{\partial g}\\ &\quad\times\left[\cos(\theta_{\rm y}) \quad \cos(\theta_{\rm y} - \tfrac{2}{3}\pi) \quad \cos\left(\theta_{\rm y} - \tfrac{4}{3}\pi\right)\right]^{\rm T}\end{aligned} \tag{23}$$

where

$$\begin{aligned}\frac{\partial B_{\rm p}}{\partial g} &= -\frac{2B_{\rm r}a_1\sinh(a_1 l_m)}{\mu_{\rm mr}\mathrm{sch}_1^2}\mathrm{sch}_1'\\ \mathrm{sch}_1' &= \mu_{\rm mr}\cosh(a_1 g)\cosh(a_1 l_m) + \sinh(a_1 g)\sinh(a_1 l_m).\end{aligned} \tag{24}$$

By substituting (4)–(9), (12), (14), (15), (22), and (23) into (19), the vertical electromagnetic force (19) is simplified or transformed as

$$\begin{aligned}F_{\rm v} &= \frac{9}{8}\frac{\partial L_{\rm ph}}{\partial g}\left[\left(i_{\rm d}^{\rm x}\right)^2 + \left(i_{\rm q}^{\rm x}\right)^2\right] + \frac{9}{8}\frac{\partial L_{\rm ph}}{\partial g}\left[\left(i_{\rm d}^{\rm y}\right)^2 + \left(i_{\rm q}^{\rm y}\right)^2\right]\\ &\quad + \frac{3}{2}Nl\frac{\partial B_{\rm p}}{\partial g}i_{\rm d}^{\rm x} + \frac{3}{2}Nl\frac{\partial B_{\rm p}}{\partial g}i_{\rm d}^{\rm y} + F_{\rm v3}\end{aligned} \tag{25}$$

where the expression of $\partial L_{\rm ph}/\partial g$ given by (21), the expression of $\partial B_{\rm p}/\partial g$ given by (24). $F_{\rm v3}$ in (25) denotes the static attraction force generated by the magnet array. Its model is as follows:

$$F_{v3} = \frac{\partial W_{\rm fa}}{\partial g} = -\frac{\mu_0 l^2}{2} \sum_{k=1,3,\ldots}^{\infty} \frac{M_k^2 \sinh^2(a_k l_m)}{{\rm sch}_k^2}. \quad (26)$$

The minus in (26) denotes that there is a static attraction force between the stator and the mover. However, $F_{\rm v}$ will tend to zero as g increases.

V. Characteristics of the Vertical Force

In the control systems of synchronous permanent-magnet rotary motors, the vector control method is used broadly. It is well known that, for maximizing the ratio of torque to current, the d-axis currents are usually kept nearly zero during the stable operation period of the SPMPM controlled by the vector control method [12]. From (17) and (18), it can be seen that the vector control method is also applicable in the SPMPM control system. Similarly, we can assume that $i_{\rm d}^{\rm x} = 0$ and $i_{\rm d}^{\rm y} = 0$ when the SPMPMs are during the stable operation period. Hence, the vertical force equation (25) can be rewritten as

$$F_{\rm v} = \frac{9}{8}\frac{\partial L_{\rm ph}}{\partial g}\left(i_{\rm q}^{\rm x}\right)^2 + \frac{9}{8}\frac{\partial L_{\rm ph}}{\partial g}\left(i_{\rm q}^{\rm y}\right)^2 + F_{\rm v3}. \quad (27)$$

Equation (27) shows that the vertical force F_v is the quadratic function of d-axis currents $i_{\rm d}^{\rm x}$ and $i_{\rm d}^{\rm y}$. Furthermore, it has been concluded in Section IV that $F_{\rm v3} < 0$. Therefore, the vertical force $F_{\rm v}$ is lesser than zero. It means that there is an attraction force between the mover and the stator of the SPMPM. Equations (25) and (27) can be used to estimate the attraction force between the mover and the stator and may be helpful for the design of the contactless planar bearing and the servo control system of the SPMPM.

For explaining the characteristics of the vertical force of SPMPM more exactly, an SPMPM which contains an Askawa's magnet array is analyzed by using (27) and (21). The parameters of this SPMPM are shown in Table I. Fig. 3 shows the variation of the vertical force in terms of the d-axis currents. For simplicity, Carter's effect is not considered in. That is $K_{\rm c1} = K_{\rm c2} = 1$. The coordination of the extreme point of the quadratic surface is (0 A, 0 A, −140 N).

A 3-D finite-element model is established by using Maxwell 3D. In this model, the teeth and slots of the armature are cancelled, i.e., the armature core is modeled as an iron plate. In addition, only one d-axis equivalent coil for every pole-pair winding is included in the FEM model. The current of the d-axis equivalent coil is equal to the d-axis current $i_{\rm q}^{\rm x}$ or $i_{\rm q}^{\rm y}$. In FEM calculation, $i_{\rm q}^{\rm x}$ is set to 0 A, 5 A, or 10 A and $i_{\rm q}^{\rm y}$ is set to 0 A, 5 A, or 10 A, respectively. Then a series of results shown in Fig. 4 are obtained. The surface generated by these FEM results has the properties of quadratic surface relative to $i_{\rm q}^{\rm y}$.

By comparing the analytical result with the FEM result, an error surface shown in Fig. 5 can be obtained. When $i_{\rm q}^{\rm x} = 0$ and $i_{\rm q}^{\rm y} = 0$, the error is equal to −10 N approximately. In addition, the relative error of the results from the analytical method

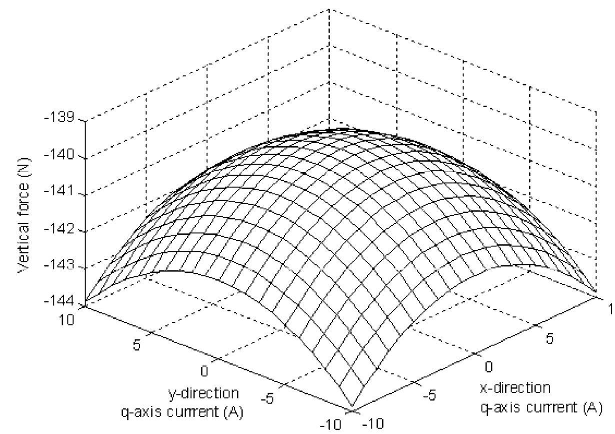

Fig. 3. Variation of the vertical force in terms of the d-axis currents.

TABLE I
Parameters of the Magnet Array and Planar Armature

Part	Item	Symbol	Unit	Value
Magnet (NdFe35)	relative permeability	$\mu_{\rm mr}$		1.10
	magnetic retentivity	$B_{\rm mr}$	T	1.23
	pitch of the array	τ	mm	10
	height	$l_{\rm m}$	mm	15
	number of turns in series per phase	$N_{\rm ph}$		100
mover/ stator core	relative permeability	$\mu_{\rm mr}$		1000
	mover core x-axis length	$l_{\rm x}$	mm	60
	mover core y-axis length	$l_{\rm y}$	mm	60
	Air-gap thickness	g	mm	2.8

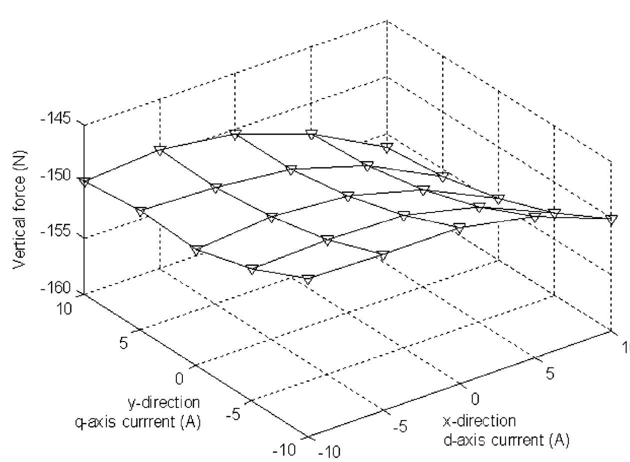

Fig. 4. Variation of the vertical force in terms of the d-axis currents which is obtained by FEM.

proposed in this paper is also evaluated. Fig. 6 shows the relative error surface. For $i_{\rm q}^{\rm x} = 0$ and $i_{\rm q}^{\rm y} = 0$, the error is equal to $-10/-150 = 6\%$. Observing Fig. 6, we can see that when $i_{\rm q}^{\rm x} < 10$ A and $i_{\rm q}^{\rm y} < 10$ A, i.e., $i_{\rm q}^{\rm x} N_{\rm ph} < 1000$ A · Turns and $i_{\rm q}^{\rm y} N_{\rm ph} < 1000$ A · Turns, the relative error is less than 10%. It can be concluded that for the ordinary current range, the results

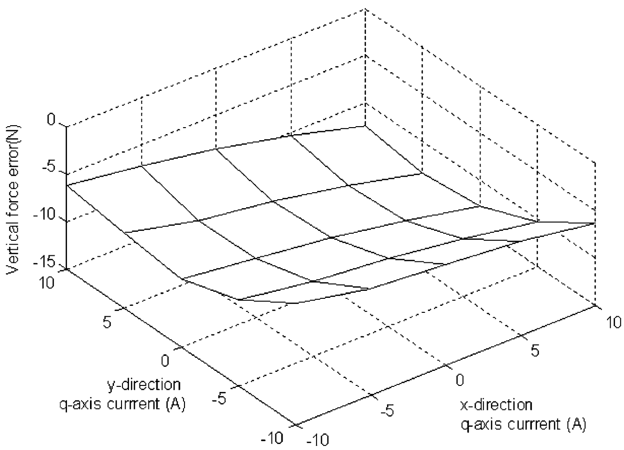

Fig. 5. Absolute error of the vertical force calculated by analytical method.

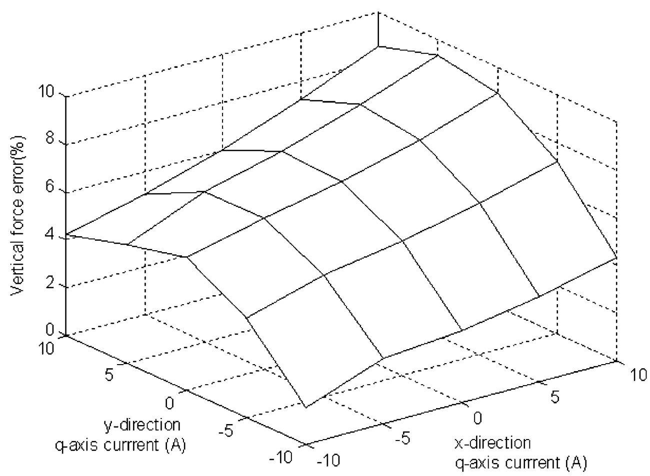

Fig. 6. Relative error of the vertical force calculated by analytical method.

obtained by the method proposed in this paper is equal approximately to the results obtained by FEM.

VI. Conclusion

The core-type SPMPM discussed in this paper is an electromechanical system including electrical parts: magnet array part, x-winding part and y-winding part, and so on. Correspondingly, the magnetic field energy in a core-type SPMPM is the result of the coupling between three electrical parts. According to electromechanical theory, a magnetic field energy equation for describing the electromagnetic coupling can be established. By using virtual work principle, x-direction thrust force, y-direction thrust force, and vertical force acting on the planar armature are modeling analytically. When the excitation flux linkages and phase currents are all transformed into d-q synchronous reference frame, a decoupling force models is obtained. From the decoupling force equations, it can be seen that the x-direction thrust force and y-direction force are the linear function of d-axis currents, and the vertical attraction force is the quadratic function of d-axis currents. The decoupling force model will be helpful for the design of the contactless planar bearing and the servo control system of the SPMPM.

Appendix

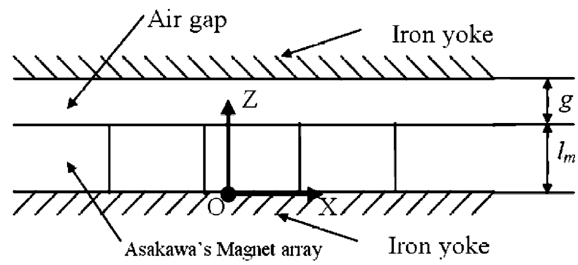

Fig. 7. Cut-view of analysis model [1].

Appendix A

A geometry model of Asakawa's magnet array is given in Fig. 7. According to Ampere's circuital law, the following scalar magnetic potential equation for Asakawa's array can be derived [1]:

$$u(x,y,z) = \sum_{k=1,3,\ldots}^{\infty} u_k(z)[\sin(a_k x) + \sin(a_k y)]$$

where $a_k = k\pi/\tau, \tau$ is the pitch of the array. $u_k\ (z)$ is a piecewise function given by

$$u_k(z) = \begin{cases} A_k \sinh(a_k z), & z \in [0, l_{\rm m}) \\ B_k e^{a_k l_{\rm gm}} \sinh[a_k(z - l_{\rm gm})], & z \in (g, l_{\rm gm}] \end{cases}. \tag{28}$$

In (28), g is the thickness of the air gap, $l_{\rm m}$ is the height of the magnet array, and $l_{\rm gm} = g + l_{\rm m}$. A_k and B_k are expressed by

$$\begin{aligned} A_k &= \frac{M_k}{2a_k}\frac{\sinh(a_k g)}{{\rm sch}_k} \\ B_k &= -\frac{M_k}{2a_k}\frac{\exp(-a_k l_{\rm gm})\sinh(a_k l_{\rm m})}{{\rm sch}_k} \\ {\rm sch}_k &= \mu_{\rm mr}\sinh(a_k g)\cosh(a_k l_{\rm m}) \\ &\quad + \cosh(a_k g)\sinh(a_k l_{\rm m}) \\ M_k &= \frac{2B_{\rm r}}{\mu_0 \pi}\frac{1}{k} \end{aligned}$$

where $\mu_{\rm mr}$ is the relative permeability of the magnets and $B_{\rm r}$ is retentivity.

The magnetic flux density vector $\boldsymbol{B}$ and the magnetic intensity $\boldsymbol{H}$ satisfies $\boldsymbol{B} = \mu_0\ \boldsymbol{H}$ and $\boldsymbol{B} = \mu_0\mu_{\rm rm}\boldsymbol{H}$ in the air gap and in the magnetic array, respectively. It is known that the magnetic intensity vector $\boldsymbol{H} = \nabla u$. Therefore, the equations for calculating the projections of $\boldsymbol{B}$ can be derived:

$$B_{\mathrm{x}} = \begin{cases} -\mu_0 \displaystyle\sum_{k=1,3,\ldots}^{\infty} a_k u_k(z)\cos(a_k x) & z \in (g, l_{\mathrm{gm}}] \\ -\mu_0\mu_{mr} \displaystyle\sum_{k=1,3,\ldots}^{\infty} a_k u_k(z)\cos(a_k x) & z \in [0, l_{\mathrm{m}}) \end{cases} \tag{29}$$

$$B_{\mathrm{y}} = \begin{cases} -\mu_0 \displaystyle\sum_{k=1,3,\ldots}^{\infty} a_k u_k(z)\cos(a_k y) & z \in (g, l_{\mathrm{gm}}] \\ -\mu_0\mu_{mr} \displaystyle\sum_{k=1,3,\ldots}^{\infty} a_k u_k(z)\cos(a_k y) & z \in [0, l_{\mathrm{m}}) \end{cases} \tag{30}$$

$$B_{\mathrm{z}} = \begin{cases} -\mu_0 \displaystyle\sum_{k=1,3,\ldots}^{\infty} F_k \frac{\partial u_{\mathrm{g}k}}{\partial z} & z \in (g, l_{\mathrm{gm}}] \\ \mu_0\mu_{\mathrm{mr}} \displaystyle\sum_{k=1,3,\ldots}^{\infty} F_k \left(\frac{M_k}{\mu_{mr}} - \frac{\partial u_{\mathrm{m}k}}{\partial z}\right) & z \in [0, l_{\mathrm{m}}) \end{cases} \tag{31}$$

where

$$\begin{aligned} F_k &= [\sin(a_k x) + \sin(a_k y)] \\ \frac{\partial u_{\mathrm{g}k}}{\partial z} &= a_k B_k e^{a_k l_{\mathrm{gm}}} \cosh[a_k(z - l_{\mathrm{gm}})] \\ &= -\frac{M_k}{2} \frac{\sinh(a_k l_{\mathrm{m}}) \cosh[a_k(z - l_{\mathrm{gm}})]}{\mathrm{sch}_k} \\ \partial u_{\mathrm{m}k}/\partial z &= a_k A_k \cosh(a_k z). \end{aligned}$$

According to the theory of magnetic field energy, the equations for calculating he magnetic field energy of permanent-magnet array W_{fa}:

$$W_{\mathrm{f}} = \frac{1}{2\mu_0}\int_{V_g} |\boldsymbol{B}|^2 \mathrm{d}V_{\mathrm{g}} + \frac{1}{2\mu_0\mu_{\mathrm{mr}}}\int_{V_m} |\boldsymbol{B}|^2 \mathrm{d}V_{\mathrm{m}}. \tag{32}$$

V_{g} and V_{m} denote the spaces of the air gap and the magnetic array, respectively. Consequently, substituting (29)–(31) into (32) yields

$$\begin{aligned} W_{\mathrm{f}} &= \sum_{k=1,3,\ldots}^{\infty} W_{\mathrm{f}k} \\ &= \sum_{k=1,3,\ldots}^{\infty} \mu_0 l^2 \left(\frac{M_k^2 l_{\mathrm{m}}}{2\mu_{\mathrm{mr}}} - \frac{M_k^2 \sinh(a_k g)\sinh(a_k l_{\mathrm{m}})}{2a_k \mathrm{sch}_k}\right). \end{aligned}$$

ACKNOWLEDGMENT

This work was supported by the National Natural Science Foundation of China under Grant 50577037 and Grant 50705060.

REFERENCES

[1] H.-S. Cho and H.-K. Jung, "Analysis and design of synchronous permanent-magnet planar motors," *IEEE Trans. Energy Convers.*, vol. 17, no. 4, pp. 492–499, Dec. 2002.

[2] H.-S. Cho, C.-H. Im, and H.-K. Jung, "Magnetic field analysis of 2-D permanent magnet array for planar motor," *IEEE Trans. Magn.*, vol. 37, no. 5, pp. 3762–3766, Sept. 2001.

[3] J. Y. Cao *et al.*, "Analysis and comparison of two-dimensional permanent-magnet arrays for planar motor," *IEEE Trans. Magn.*, vol. 40, no. 6, pp. 3490–3494, Nov. 2004.

[4] J. De Boeij, E. Lomonova, and A. Vandenput, "Modeling ironless permanent-magnet planar actuator structures," *IEEE Trans. Magn.*, vol. 42, no. 8, pp. 2009–2016, Aug. 2006.

[5] J. Y. Cao *et al.*, "A novel synchronous permanent magnet planar motor and its model for control application," *IEEE Trans. Magn.*, vol. 41, no. 6, pp. 2156–2163, Jun. 2005.

[6] J. C. Compter, "Electro-dynamic planar motor," *Precision Engineering*, vol. 28, pp. 171–180, 2004.

[7] T. Ueta, B. Yuan, and T.-C. Teng, "Moving Magnet Type Planar Motor Control," U.S. Patent 2003/0102722, Jan. 2003.

[8] T. Ueta and B. Yuan, "Moving Coil Type Planar Motor Control," U.S. Patent 2003/0102721, Jan. 2003.

[9] A. J. Hazelton, M. B. Binnard, and J.-M. Gery, "Electric Motors and Positioning Device Having Moving Magnet Arrays and Six Degrees of Freedom," U.S. Patent 6208045, 2001.

[10] A. J. Hazelton and J. M. Gery, "Planar Electric Motor and Positioning Device Having Transverse Magnets," U.S. Patent 6285097, 2001.

[11] J. R. Hendershot, Jr. and T. J. E. Miller, *Design of Brushless Permanent-Magnet Motors*. Oxford, U. K.: Magna Physics Publishing and Clarendon Press, 1994.

[12] R. Y. Tan, *Modern Permanent Magnet Machines: Theory and Design* (in Chinese). China: Mechanical Industry Press, 1997.

[13] R. Huang, J. Zhou, and G. T. Kim, "Minimization design of normal force in synchronous permanent magnet planar motor with Halbach array," *IEEE Trans. Magn.*, vol. 44, no. 6, pp. 1526–1528, Jun. 2008.

Jiayong Cao received the B.S. and M.S. degrees from Fuzhou University, Fuzhou, China, in 1995 and 1998, respectively, and the Ph.D. degree from Huazhong University of Science and Technology, Wuhan, China, in 2003.

From 2004 to 2006, he was a post doctor of the Institute of Manufacturing Engineering, Department of Precision Instruments and Mechanology, Tsinghua Unviersity, Beijing, China. Since 2006, he has been an Assistant Professor in the School of Mechanical Engineering, Shanghai Jiao Tong University, Shanghai, China. His research interests include mechatronics, magnetic levitation stage, and motion control.